

**SIMULATION OF AURORAL PHOTOEMISSION RATE FOR THE
FIRST NEGATIVE BAND SYSTEM OF N_2^+ AT λ 427.8 nm
USING ELECTRON DIFFERENTIAL NUMBER FLUX
OBSERVED BY THE SOUNDING ROCKET**

**Kunizo ONDA^{1,2}, Hiroshi MIYAOKA³, Yukikazu ITIKAWA²
and Masaki EJIRI³**

¹*Faculty of Industrial Science and Technology, Science University of Tokyo,
Oshamambe, Yamakoshi-gun, Hokkaido 049-35*

²*Institute of Space and Astronautical Science, Yoshinodai, Sagami-hara 229*

³*National Institute of Polar Research, Kaga 1-chome, Itabashi-ku, Tokyo 173*

Abstract: Electron auroras observed by the sounding rocket S-310JA-8 are investigated by using the Monte Carlo method. The MSIS-86 model is employed to represent the atmospheric number density and temperature in the aurora observed at Syowa Station in Antarctica of the invariant latitude 66.14°S and the geomagnetic longitude 70.98° on April 4, 1984. Only N_2 , O and O_2 are taken into account as components of the atmosphere. Electrons are injected downward into the upper atmosphere at the altitude of 200 km, at which a downward electron differential number flux was measured. An initial electron energy E_0 is considered in the range of 100 eV to 18 keV. It is assumed that an initial pitch angle is uniformly distributed in the range of $[0, \pi/2]$. Production and emission at λ 427.8 nm rates of the first negative band system of nitrogen molecular ions N_2^+ ($B^2\Sigma_u^+$) are calculated as a function of altitude, the initial pitch angle, and the initial electron energy. Time variation of the observed absolute intensity of this line is reasonably well reproduced by the Monte Carlo method combined with the measured electron number flux. The difference in the absolute intensities obtained by experiment and theory is 5% at the time $X + 216$ s. This confirms that the Monte Carlo method is applicable to simulate collision processes and the resulting production and emission rates in electron auroras. Some representative results of emission rates are also presented for oxygen green and red lines.

1. Introduction

The sounding rocket S-310JA-8 was launched successfully from Syowa Station in Antarctica (the invariant latitude 66.14°S , the geomagnetic longitude 70.98° , the magnetic local time being nearly equal to the universal time) at 1927:01 (UT) on April 4, 1984 toward active auroral arcs at a substorm expansion phase. The observational results were reported in detail by EJIRI (1988) and EJIRI *et al.* (1988a, b,c). In this rocket experiment, the aurora images were taken every 5.62 s in a visible range from about λ 400 to λ 800 nm by using a visible auroral television (VAT) camera. The absolute value of emission intensity at the center of the camera

image was monitored by a photometer, in which an interference filter was used for the wavelength of λ 427.8 nm emitted from the first negative band system of N_2^+ . An energy spectrum of particles (electrons in this experiment) was measured by a quadrispherical electrostatic spectrometer in the range from 16 eV to 14.4 keV. Number density of thermal electrons produced by precipitating energetic electrons, which collide with neutral atoms and molecules in the atmosphere, was measured by a sweep frequency impedance probe with the frequency range up to 10 MHz and a sweep period of 0.5 s.

There are many model calculations on electron transport and energy deposition of auroral electrons, for example, REES (1963), BANKS *et al.* (1974), STRICKLAND *et al.* (1976), SOLOMON *et al.* (1988), and LINK (1992), and some review papers related to electron auroras written by REES (1969), REES and ROBLE (1975), TORR and TORR (1982), REES (1987), and SOLOMON (1991).

As one of plausible model calculations, the Monte Carlo method has been applied to electron transport problems related to electron auroras by BERGER *et al.* (1970), CICERONE and BOWHILL (1971), JACKMAN and GREEN (1979), and very recently SOLOMON (1993) and SERGIENKO and IVANOV (1993). These studies have employed empirically fitted formulas (JACKMAN and GREEN, 1979; YUROVA and IVANOV, 1989) for the electron scattering cross sections from N_2 , O_2 , and O gases.

It is very interesting for us to test quantitatively accuracy of the Monte Carlo method. We focused our attention to the active auroral arcs observed by the sounding rocket at Syowa Station in Antarctica. We employed the Monte Carlo method to simulate collision processes of precipitating electrons with the atmospheric particles, production and emission rates of oxygen green and red lines and the first negative band system of N_2^+ . The downward electron differential number flux, which is shortly stated in the following as the electron differential flux, was measured at Syowa Station on the same sounding rocket experiment, and is used to make a relative intensity of emission rates into the absolute value.

In this paper, we assumed that the electrons start precipitating downward at the height of 200 km, a pitch angle distribution of them is uniform in the range of $[0, \pi/2]$, and constituent elements of the upper atmosphere at Syowa Station are N_2 , O, and O_2 . The number densities of the atmospheric particles are estimated by using the MSIS-86 model of HEDIN (1983, 1987). The data sets of the collision cross sections between electrons and N_2 , O, and O_2 are adopted from the data compilations by ITIKAWA *et al.* (1986, 1989) and ITIKAWA and ICHIMURA (1990). Results of the Monte Carlo calculations are sensitive to the cross sections employed, specifically for excitation processes with low excitation energies such as those of $O(^1D)$ and $O(^1S)$. In order to revise the data set for the O atom, we substituted in part the excitation cross sections of $O(^1D)$ and $O(^1S)$ experimentally determined by DOERING and GULCICEK (1989) and DOERING (1992). In the low energy region, we employed specifically digitized data, as detailed as possible for the cross sections. We plan to report the dependence of the resulting excitation rates on the cross sections employed.

A brief outline of our method is described in the next section (see ONDA *et al.*,

1992, in detail). The magnetic line of force is regarded as straight within the range of altitude from 80 to 200 km. After examining the dependence of excitation and emission rates on magnitude of a magnetic flux density between 30000 and 50000 nT, magnitude of the magnetic flux density is taken to be 43000 nT. The angle β between the local line of force and the vertical line is set to be 25° .

Numerical results are presented and discussed in Section 3. We calculated the absolute intensity of the photons emitted from the first negative band system of N_2^+ at the wave length of λ 427.8 nm, and compared time variation of the absolute intensity of λ 427.8 nm deduced from the sounding rocket experiment reported by EJIRI (1988) and EJIRI *et al.* (1988b) with that obtained by using the Monte Carlo method combined with the measured electron differential flux. This theoretical absolute intensity agrees with the experimental one within difference of 5–30% for the period between $X+208$ s and $X+220$ s, though the theory overestimates the experimental value by a factor of 2.7 at $X+193$ s, and underestimates by 0.5 at $X+226$ s.

We estimated also the production and emission rates of oxygen green and red lines and presented them in Section 3. These results give us some ideas on the absolute values of emission rates of these familiar oxygen lines. Concluding remarks are stated in Section 4.

2. Calculations

Geomagnetic lines of force are regarded as approximately straight in the altitude range from 80 to 200 km. The z axis of our coordinate system is taken along the line of force. Motion of an electron between collisions with the atmospheric particles is determined by solving the classical equation of motion under the assumption that only the geomagnetic field causes the Lorentz force on the electron. The effect of any electric field on the electron motion is disregarded in this study. SI units are used throughout this paper unless otherwise stated.

The following four procedures are carried out in the Monte Carlo calculations by using random numbers created on a computer: (A) *decision of occurrence of collision*; (B) *decision of type of collision target*; (C) *decision of type of collision process*; and (D) *decision of the scattering direction*. The details of these procedures are described in the ISAS report by ONDA *et al.* (1992).

The MSIS-86 model is adopted to represent atmospheric number densities and temperatures for aurora observed at the invariant latitude 66.14° and the geomagnetic longitude 70.98° on April 4, 1984. Only N_2 , O and O_2 are taken into account in this work. The number densities of these elements are shown in Fig. 1. The exospheric temperature is $T_{ex} = 1170.28$ K, and other parameters in this model are set as follows: $F107 = 129.0$; $F107A = 125.1$; and $Ap = 84.0$.

The energy loss for an elastic collision is given by the momentum-transfer loss $\Delta E = (2m/M_j)(1 - \cos \omega) E_i$; where m is the mass of the electron, M_j is that of the j th atmospheric particle, ω is the scattering angle, and E_i is the energy of the electron before the collision. The electron energy after an inelastic collision is given

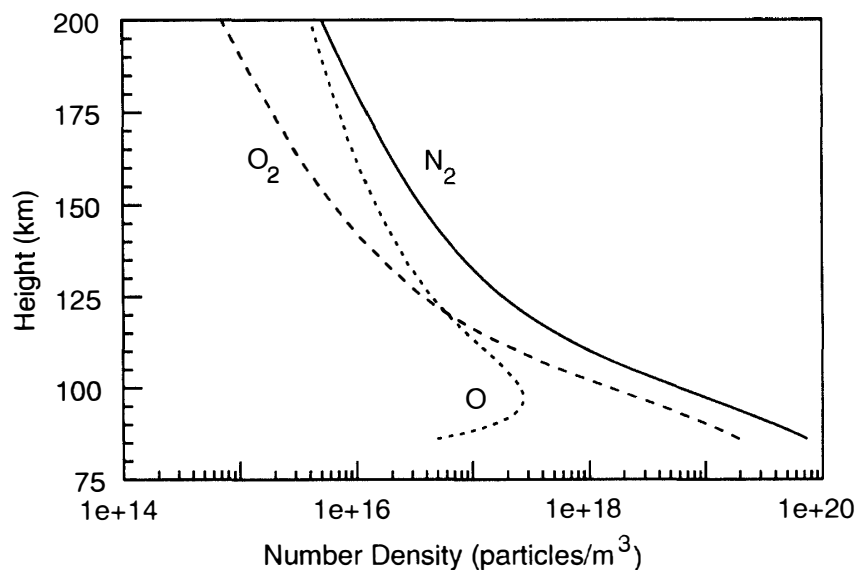


Fig. 1. Altitude dependence of number densities of N_2 , O and O_2 at Syowa Station on April 4, 1984 estimated by the MSIS-86 model atmosphere.

by $E_f = E_i - \Delta E$, where ΔE is the energy loss in the collision. The energy loss for an ionizing collision is the sum of the relevant ionization energy and the kinetic energy of the secondary electron.

In addition to the momentum transfer in elastic collisions, the excitation of discrete levels and ionization with or without excitation of residual ions are considered for each neutral component of the atmosphere. Three electronic states of N_2^+ are distinguished in ionizing collisions of N_2 . For O and O_2 , however, we did not distinguish the ion states. When the target is a molecule, N_2 or O_2 , we use an approximate analytic expression for the energy distribution of secondary-electrons (OPAL *et al.*, 1971, 1972). For atomic oxygen, we have no experimental data for the energy distribution of secondary-electrons. We use the same analytic expression as for O_2 . The number of states taken into account in this work is 16 for N_2 , 11 for O , and 8 for O_2 (see ONDA *et al.*, 1992, in detail). The values of the relevant cross sections used in this work are those reported in the data reviews by ITIKAWA *et al.* (1986, 1989), and by ITIKAWA and ICHIMURA (1990). For excitation cross sections of $O(^1D)$ and $O(^1S)$ we have examined in part experimental values determined by DOERING and GULCICEK (1989) and DOERING (1992). Details of these results will be reported in another publication.

The energy loss of the precipitating electrons due to collisions with ambient ionospheric electrons is neglected in this work. This is permissible at least in the energy range above 2 eV, because the rate of energy loss is estimated to be 5×10^{-5} eV/m for E (energy of precipitating electrons) = 5 eV, T_e (temperature of ambient ionospheric electrons) = 300 K, and N_e (number density of ambient electrons) = 10^{12} m^{-3} , and that of excitation of atoms and molecules in the atmosphere is the order of 10^{-3} eV/m, which is estimated from a representative stopping cross section of electrons times a representative number density of atmospheric particles.

3. Results and Discussion

Calculations have been carried out under the following initial conditions of precipitating electrons: (1) the electrons are injected downward into the atmosphere at an altitude of $h_0=200$ km, at which the electron differential flux was measured by the sounding rocket experiment; (2) the energy of precipitating electrons is investigated in the range of $E_0=0.1-18$ keV, and if the electron energy falls below 2 eV, tracing of the electron is stopped; (3) a pitch angle α_0 , which is the angle between an initial electron velocity and the geomagnetic line of force, is taken in the range of $\alpha_0=0-90^\circ$ (as will be shown later, results for $\alpha_0=90^\circ$ will be safely replaced by those for $\alpha_0=80^\circ$); and (4) the angle β between the local line of force and the vertical, is set to be $\beta=25^\circ$. These values are chosen from consideration of actual electron auroras observed at Syowa Station.

3.1. A magnetic field dependence of production and emission rates

An IGRF 90 model is employed to estimate magnitude of a magnetic flux density. Estimated values are 40274 nT at an altitude of 250 km, 41070 nT at 200 km, and 42723 nT at 100 km at 1927:01 (UT) on April 4, 1984 at Syowa Station. We examined the dependence of production and emission rates on magnitude of the magnetic flux density, because the Larmor radius of the electron is inversely proportional to the magnetic flux density and thus it is possible for the electron to change its traveling distance and therefore frequency of collisions with the atmospheric particles. Our results show that the production rates of excited states, such as $N_2^+(\text{B}^2\Sigma_u^+)$, $O(^1D)$, and $O(^1S)$ are almost independent of strength of the magnetic flux density within the range of 30000–50000 nT.

Therefore, we take the magnetic flux density to be 43000 nT in the following study. The reason is that our main concern of this study is to estimate the absolute intensity of λ 427.8 nm emitted from the first negative band system of N_2^+ , and its peak height of such emission is about 90–120 km in the range of the initial electron energy of 0.1–18 keV.

3.2. Initial electron pitch angle and energy dependence of production and emission rates

In this study, the production of excited states of the atmospheric constituents N_2 , O, and O_2 is caused solely through collisions with precipitating electrons. We consider the representative auroral emission from the excited states of $N_2^+(\text{B}^2\Sigma_u^+)$, $O(^1D)$, and $O(^1S)$. The radiative lifetime of these excited states is known to be 60×10^{-9} s, 147 s, and 0.79 s, respectively. Since it is possible for the excited states of $O(^1D)$ and $O(^1S)$ to be collisionally quenched before emission of photons, in order to estimate the emission rates of the oxygen red and green lines, we have taken into account collisions of these excited O atoms with N_2 and O_2 molecules under the neutral gas temperature in the altitude range of 80–200 km (see STREIT *et al.*, 1976; TAKAYANAGI, 1984; ONDA *et al.*, 1992, in detail).

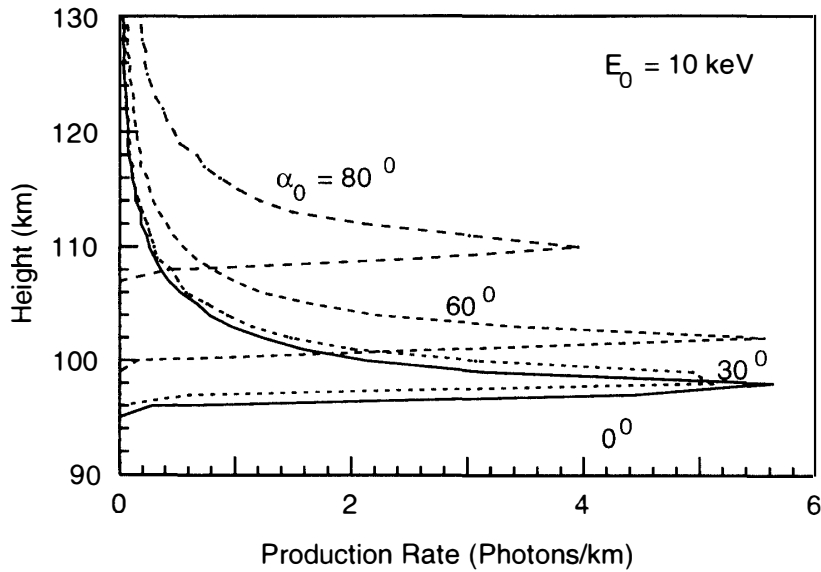


Fig. 2. Altitude dependence of production rates of $N_2^+(B^2\Sigma_u^+)$ per primary electron as a function of the initial pitch angle at $E_0 = 10$ keV.

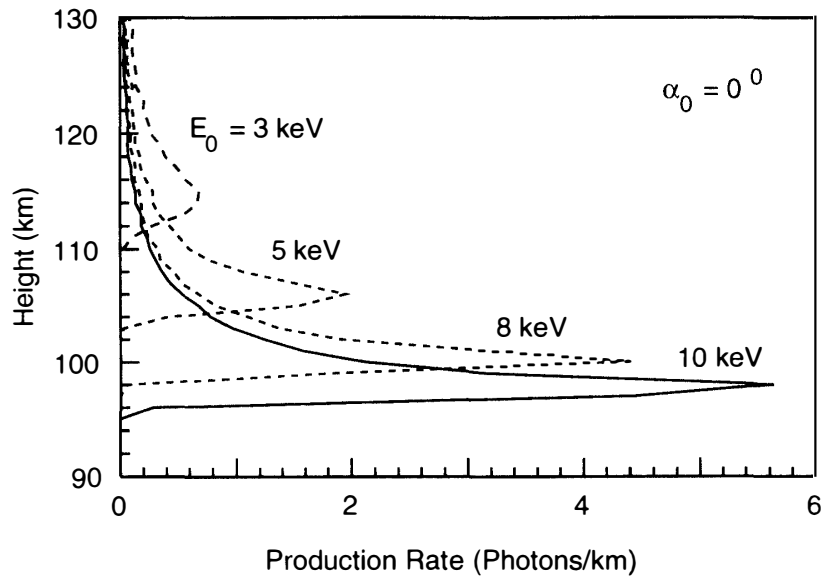


Fig. 3. Altitude dependence of production rates of $N_2^+(B^2\Sigma_u^+)$ per primary electron as a function of the initial electron energy E_0 for $\alpha_0 = 0^\circ$.

Production rates of $N_2^+(B^2\Sigma_u^+)$ per primary electron are shown in Fig. 2 as a function of the initial pitch angle at the initial electron energy $E_0 = 10$ keV, and they are shown in Fig. 3 as a function of the initial electron energy for the pitch angle $\alpha_0 = 0^\circ$. This emission is produced mainly by primary electrons. The emission rate is in the range of 0.5–6 photons/km. As can be seen from Fig. 2, the production rates of N_2^+ are almost insensitive to the pitch angles in the range of 0 – 60° , and the same is true for ionization rates of O_2 molecules. But, according as the pitch angle becomes larger than 60° , the peak height of production rates of molecular ions shifts upwards about a few tens km and therefore the peak value of the production rates

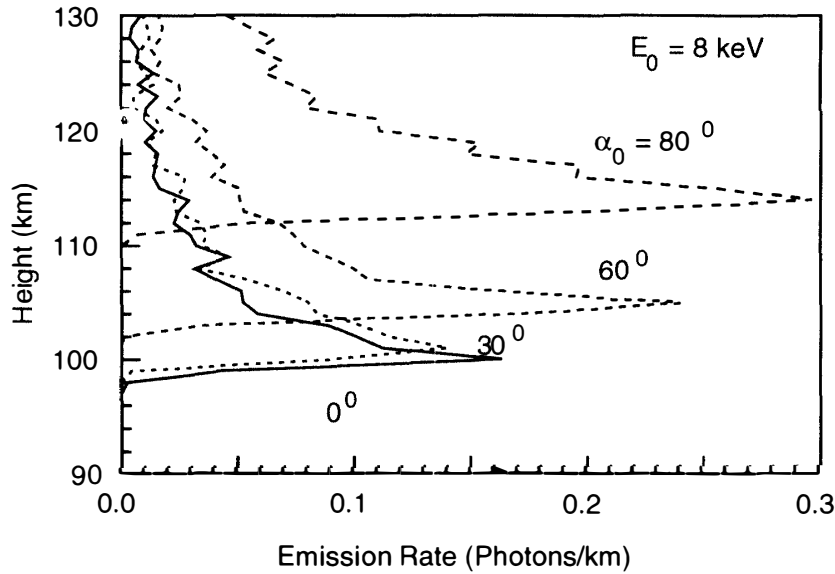


Fig. 4. Altitude dependence of the photon emission of the oxygen green line at $\lambda 557.7 \text{ nm}$ per primary electron as a function of the initial pitch angle at the initial electron energy $E_0 = 8 \text{ keV}$.

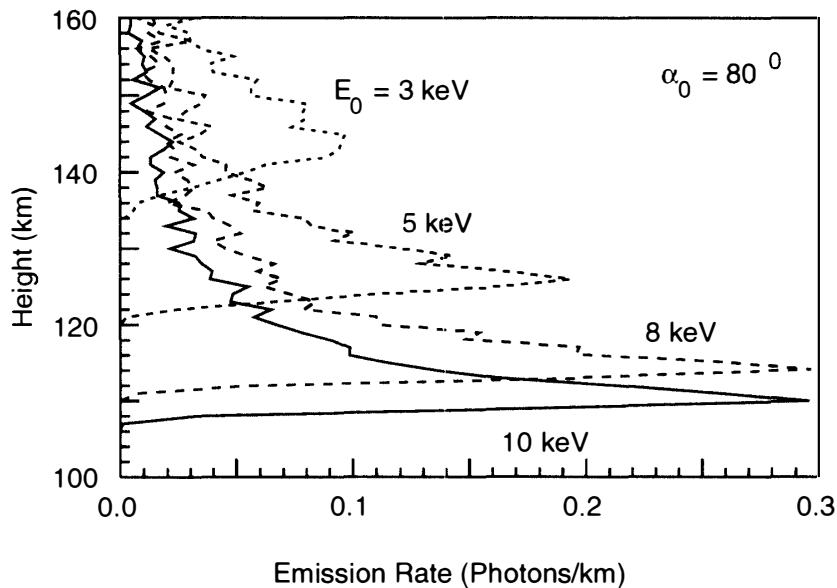


Fig. 5. Altitude dependence of the photon emission of the oxygen green line at $\lambda 557.7 \text{ nm}$ per primary electron as a function of the initial electron energy E_0 for the initial pitch angle $\alpha_0 = 80^\circ$.

becomes smaller by about 30% of the values for $\alpha_0 = 0-60^\circ$. The production rates of $\text{N}_2^+(\text{B}^2\Sigma_u^+)$ still increase and the peak height becomes lower as the incident electron energy becomes higher for any values of the pitch angle α_0 . These results are understood if we take into account two factors, that is, the first is that the electrons having higher initial energies can reach a lower region of the atmosphere and the second is that the number density of N_2 molecule continues to increase as

the altitude goes down to about 80 km.

In our calculations, many other excited states of N_2 , O, and O_2 are produced by the precipitating electrons. We show below representative results to give some ideas on magnitude of production rates of the important excited states in the electron auroras. The number of emission of the oxygen green line at λ 557.7 nm per primary electron is presented in Fig. 4 as a function of the initial pitch angle at the initial electron energy $E_0 = 8$ keV and that is shown in Fig. 5 as a function of the initial electron energy for the pitch angle $\alpha_0 = 80^\circ$. By taking into account both the radiative lifetime of the upper state $O(^1S)$ being 0.79 s and the number densities of the components of the atmosphere shown in Fig. 1, it is understood that the collisional quenching effect is small for this emission at the altitude above 110 km. This emission is predominantly caused by the secondary electrons as the previous studies of ONDA *et al.* (1992) and ONDA and ITIKAWA (1995) have shown. The most important emission region is higher than that for the first negative band system of N_2^+ by only about 10–20 km, although the excitation mechanism is completely different in these two emission processes. The emission rate is in the range 0.1–0.3 photon/km as can be seen from Figs. 4 and 5. It was pointed out by MEYER *et al.* (1969) and PARKINSON and ZIPF (1970) and has been investigated quantitatively by GATTINGER *et al.* (1985), GERDJIKOVA and SHEPHERD (1987), and SHEPHERD *et al.* (1995) that the major production process of $O(^1S)$ can be $N_2(A^3\Sigma_u^+) + O(^3P) \rightarrow N_2(X^1\Sigma_g^+) + O(^1S)$. Since the abundance of $N_2(A^3\Sigma_u^+)$ is not known at Syowa Station on April 4, 1984, we do not present a production rate of $O(^1S)$ through this process.

The number of emission of the oxygen red line at λ 630.0 nm per primary electron is shown in Fig. 6 as a function of the pitch angle at the initial electron

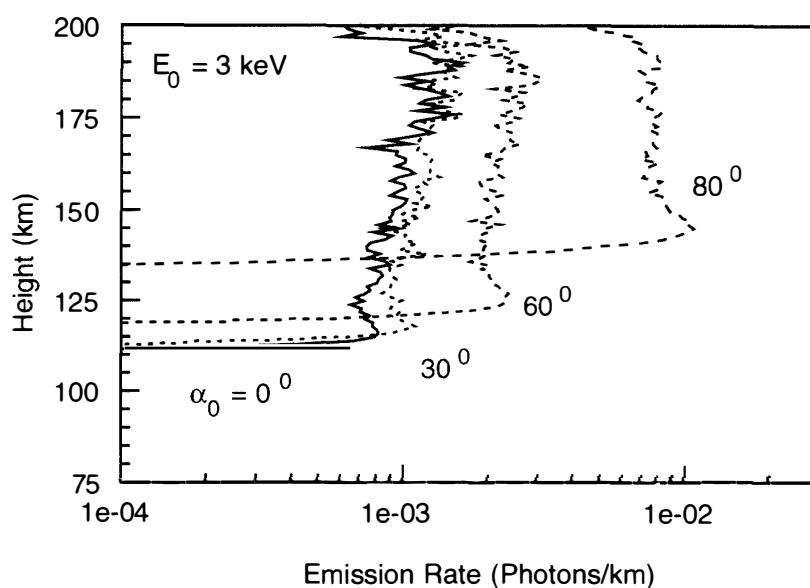


Fig. 6. Altitude dependence of the photon emission of the oxygen red line at λ 630.0 nm per primary electron as a function of the initial pitch angle α_0 at the initial electron energy $E_0 = 3$ keV.

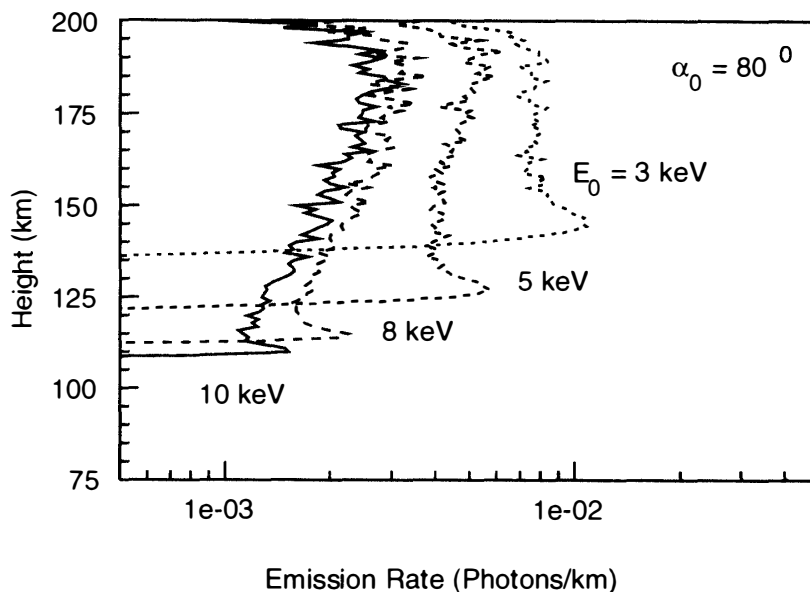


Fig. 7. Altitude dependence of the photon emission of the oxygen red line at λ 630.0 nm per primary electron as a function of the initial electron energy E_0 for the initial pitch angle $\alpha_0=80^\circ$.

energy $E_0=3$ keV, and that is displayed in Fig. 7 as a function of the initial electron energy for the pitch angle $\alpha_0=80^\circ$. In this emission, the secondary electrons also play a major role in producing this excited state. As can be seen from Fig. 6, if the incident energy is as low as $E_0=3$ keV, the red line is emitted at altitude above 150 km. The emission rate is in the range $(2-7) \times 10^{-3}$ photons/km at the altitude of 110–200 km.

As the pitch angle is increased from 0° to 90° , precipitating electrons will lose their energy more quickly at the higher altitude compared with the case of $\alpha_0=0^\circ$. Therefore, the excited state $O(^1D_2)$ will emit the red line without appreciable collisional quenching compared with the case of $\alpha_0=0^\circ$, and this behavior is understood by looking at Figs. 6 and 7.

The electron differential flux shown in Fig. 8 below tells us that electrons having energy of several hundreds eV can contribute mainly to producing the red line emission and the main emission region can be higher than 150 km. It is clearly higher than the emission region of the first negative band system of N_2^+ and also the one of the green line. Unfortunately, there is no results for the green and red lines from oxygen atoms at this experiment. Thus, we do not discuss further on the green and red line emissions from oxygen atoms at this aurora.

3.3. Comparison of theoretical estimation with observed results of the absolute intensity of λ 427.8 nm

Here, we briefly mention the sounding rocket experiments carried out at Syowa Station in Antarctica. A visible auroral television (VAT) camera was installed to take an auroral picture downwards from the spinning rocket. The photometer (PHO) was on board to measure a column volume emission rate at λ 427.8 nm in

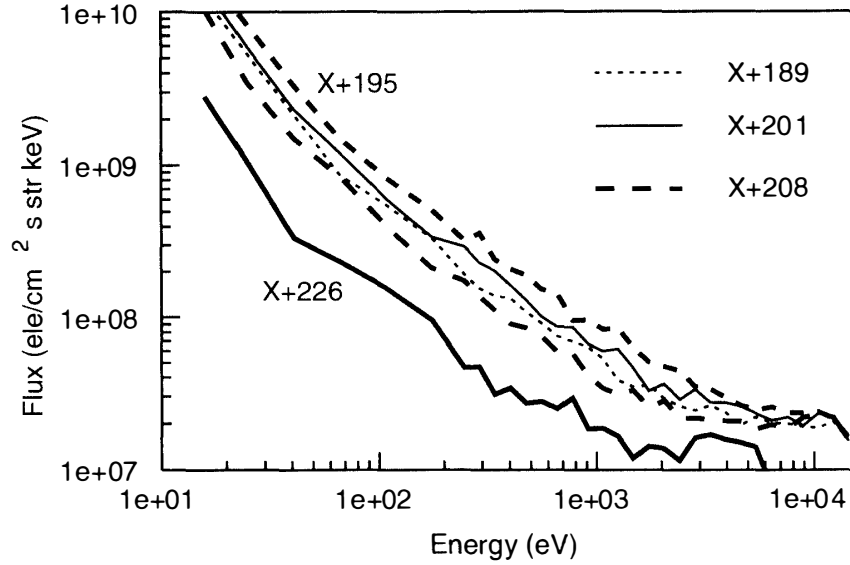


Fig. 8. Electron differential flux as a function of the electron energy observed at the sounding rocket S-310JA-8 at Syowa Station on April 4, 1984. The thin dotted line is the value at the time $X+189$ s, the thick broken line the one at $X+195$ s, the solid line the one at $X+201$ s, the thick long broken line the one at $X+208$ s and the thick solid line the one at $X+226$ s.

the first negative band system of N_2^+ ($B^2\Sigma_u^+$). Both the VAT camera and the PHO were set along the rocket spin axis. The measured value (denoted as A_1 kR) of the PHO corresponds to an emission rate (B_1 , which is the panchromatic value for $\lambda\lambda$ 400–800 nm) at the center in the VAT images. Thus, in order to calibrate the absolute value (A_2 kR) of emission intensity at the foot point of the geomagnetic field (through the rocket position) in the VAT images, it is assumed that the spectrum of the auroral emission is the same within the VAT field view. That is, A_2 is deduced from $A_1 \times B_2/B_1$ where B_2 is the VAT value at the geomagnetic foot point. This A_2 is compared with the theoretically estimated emission rate, because the measured particles produce the photoemission along the geomagnetic field.

Since energetic electrons primarily precipitate along the geomagnetic field line and produce an auroral emission, it is essential for a foot point of the geomagnetic field line through the rocket position to stay within the VAT field view. Although we launched three sounding rockets along the geomagnetic field line, only one rocket, *i.e.* (S-310JA-8) satisfied this observation condition during the flight.

The experimental values at λ 427.8 nm were recorded during the time interval of 189–226 s after the launch. At this period, the rocket was in an ascending phase. Therefore, time variation of the experimental absolute intensity at λ 427.8 nm will be compared with the theoretical one during this period in the following.

In Fig. 8, the electron differential flux $j(E)$ at time $T=X+189$, $X+195$, $X+201$, $X+208$, or $X+226$ s is plotted as a function of energy in the range of 16 eV to 14.4 keV. The flux for the energy higher than 14.4 keV was obtained by an extrapolation with using a formula $j(E)=j(E=12.25 \text{ keV})(E(\text{in keV})/12.25)^{-5.2}$, which is deduced from the high energy part of the similar energy flux at time $T=$

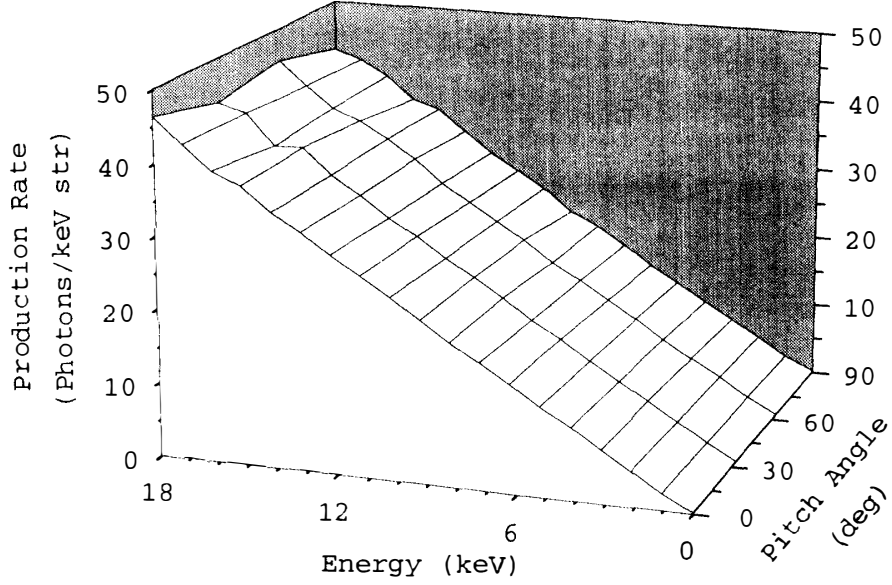


Fig. 9. Production rates of the first negative band system of N_2^+ ($B^2\Sigma_u^+$) per primary electron as functions of both the initial pitch angle and electron energy.

$X+220$ s. The production and emission rates of photons at λ 427.8 nm from N_2^+ ($B^2\Sigma_u^+$) are calculated in the range of initial electron energy of $E_0=0.1-18$ keV for the pitch angles of 0° , 30° , 60° , and 80° . One of production rates is displayed in Fig. 3 above. In order to obtain production rates as a function of both the initial electron energy and pitch angle, a height distribution of production rates is integrated over the height and the results denoted by $g(\alpha; E)$ are presented in Fig. 9, which shows that the production rates are almost independent of the pitch angle and continue to increase in magnitude according as the energy of precipitating electrons becomes higher. Integration of these production rates over the pitch angle is done as follows:

$$g(E) = 2\pi \int_0^{\pi/2} g(\alpha, E) \sin \alpha \, d\alpha = 2\pi \int_0^1 g(z, E) \, dz$$

$$\simeq \frac{\pi}{2} \left[g(z=0, E) + g\left(z = \frac{1}{2}, E\right) + g\left(z = \frac{\sqrt{3}}{2}, E\right) + g(z \simeq 1, E) \right].$$

Here, we assume that the pitch angle distribution is uniform in the range of $[0, \pi/2]$. Since the production rates are almost independent of the pitch angle of precipitating electrons, it does not matter what the assumption of a pitch angle distribution is.

The absolute value of emission rate at λ 427.8 nm in the first negative band system of N_2^+ ($B^2\Sigma_u^+$) is calculated per primary electron by using the production rates shown in Fig. 9. Since the Franck-Condon factor is known to be 0.262 as compiled by GILMORE *et al.* (1992) for the photon emission of λ 427.8 nm, we obtain the absolute strength of this emission as $0.262 \times 10^{-6} \times \int_{E_{\min}}^{E_{\max}} j(E) g(E) \, dE$ Rayleighs, where $j(E)$ is the electron differential flux measured by the sounding rocket experiment. We extend calculations up to the initial electron energy of 18 keV. Since the electron differential flux sufficiently drops beyond 18 keV as can be

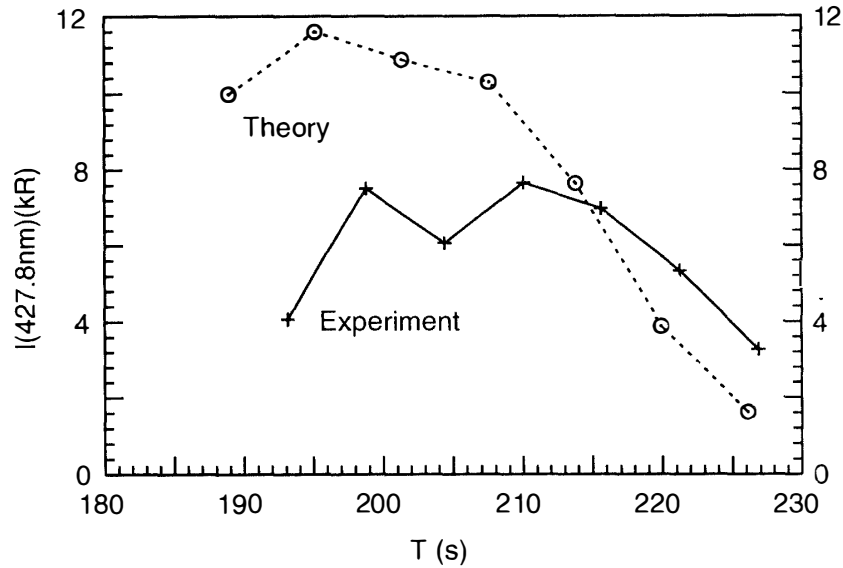


Fig. 10. The absolute intensity of photon emissions at λ 427.8 nm in the first negative band system of $N_2^+(B^2\Sigma_u^+)$ as a function of time. Experimental values are shown by a symbol + connected by a solid line and theoretical ones a circle \odot connected by a dotted line.

understood from the extrapolation formula shown above, the contribution from the energy region above 19 keV to the emission rate at λ 427.8 nm from $N_2^+(B^2\Sigma_u^+)$ is estimated to be less than a few percent.

Since the electron differential flux changes in time as shown in Fig. 8 and the activity of auroras also changes in time, emission rates depend on the electron differential flux employed. In Fig. 10, the theoretical absolute intensity of this line is compared with the value deduced from the sounding rocket experiment by EJIRI (1988) and EJIRI *et al.* (1988b, c) as a function of time after launching the rocket. Theoretical values are calculated at the time, when the electron differential flux was measured. On the other hand, the experimental values are based on the times, when the absolute intensities were measured. There is some time lag between them. As can be seen from Fig. 10, time variation of absolute intensity is reasonably reproduced by Monte Carlo calculations combined with the measured electron differential flux except for the period before $X+204$ s, where a ratio of theory to experiment is about 1.5–2.7. It is difficult for us to understand decrease in the absolute intensity at $X+204$ s observed by the experiment, because the electron differential flux measured by the same sounding rocket experiment did not change so much as shown in Fig. 8 for the period between $X+189$ s and $X+208$ s. The difference in the absolute intensity obtained by experiment and theory is within 5–30% for the period between $X+208$ s and $X+226$ s.

This reasonable agreement in the absolute intensity between the experiment and theory encourages us to apply the Monte Carlo method to electron auroras.

4. Concluding Remarks

We report here the results of simulation of collision processes of precipitating electrons with the atmospheric particles and emission processes in electron auroras observed by the sounding rocket experiment by using the Monte Carlo method. Our absolute intensity of λ 427.8 nm emitted from the first negative band system of N_2^+ is reasonably in accord with the result deduced from the sounding rocket experiment. Thus, we can safely conclude that the Monte Carlo method is applicable to simulate collision processes and resulting production and emission rates in electron auroras.

The comparison in the absolute intensity as shown in Fig. 10 clearly shows some inconsistency in the measurement of the absolute intensity of λ 427.8 nm and the electron differential flux with respect to time variation. Thus, it is highly desirable to determine experimentally the cause (the electron differential flux) and the effect (the absolute intensity of auroral emission) within the same accuracy.

We mention some points encountered in this theoretical study. First of all, Monte Carlo calculations become difficult according as the initial electron energy is increased higher. The reason is that the ionization process produces electrons more and more as the initial electron energy is increased, and tracing of these electrons becomes very time consuming in cases of initial energy higher than 8 keV. The second point is that cross sections between electrons and N_2 , O, and O_2 are not perfect yet for the moment, and should be revised over a wide range of electron energies.

The height distribution of thermal electron number density was also measured at the same sounding rocket experiment. It is possible for us to estimate the electron number density in our method, although the initial electron energy should be extended to a lower region to say 20 eV, because the electron number flux becomes greater there. We have a plan to report such results soon.

It is possible for us to estimate the production rates of $O(^1D_2)$ and $O(^1S)$. There are other production mechanisms of the excited state $O(^1D_2)$, such as dissociation of oxygen molecules by electron impact and dissociative recombination of oxygen molecular ions. As we stated in Section 3.2 above, it has been known that other production mechanisms of excited state $O(^1S)$ exist. A quantitative study of the effect of these processes on the electron aurora observed at Syowa Station is under planning.

Acknowledgments

This work is one of the cooperative projects at NIPR. Numerical calculations have been done on the FACOM VPP-500 at the Computer Center, ISAS. One of the authors (K. O.) expresses his sincere thanks for the computer resource budget to the Center for Planning and Information Systems at ISAS.

References

- BANKS, P. M., CHAPPELL, C. R. and NAGY, A. F. (1974): A new model for the interaction of auroral electrons with the atmosphere: Spectral degradation, backscatter, optical emission and ionization. *J. Geophys. Res.*, **79**, 1459–1470.
- BERGER, M. J., SELTZER, S. M. and MAEDA, K. (1970): Energy deposition by auroral electrons in the atmosphere. *J. Atmos. Terr. Phys.*, **32**, 1015–1045.
- CICERONE, R. J. and BOWHILL, S. A. (1971): Photoelectron fluxes in the ionosphere computed by a Monte Carlo method. *J. Geophys. Res.*, **76**, 8299–8317.
- DOERING, J. P. (1992): Absolute differential and integral electron excitation cross sections for atomic oxygen. 9. Improved cross section for the $^3P \rightarrow ^1D$ transitions from 4.0 to 30 eV. *J. Geophys. Res.*, **97**, 19531–19534.
- DOERING, J. P. and GULCICEK, E. E. (1989): Absolute differential and integral electron excitation cross sections for atomic oxygen. 7. The $^3P \rightarrow ^1D$ and $^3P \rightarrow ^1S$ transitions from 4.0 to 30 eV. *J. Geophys. Res.*, **94**, 1541–1547.
- EJIRI, M. (1988): Results of Sounding Rocket Experiments at Syowa Station, Antarctica, 1984. Upper Atmosphere Division, National Institute of Polar Research, Japan, 261 p.
- EJIRI, M., FUKUNISHI, H., ONO, T., YAMAGISHI, H., HIRASAWA, T., KIMURA, I. and OGUTI, T. (1988a): Auroral phenomena observed by the sounding rockets S-310JA-8 to -12 at Syowa Station, Antarctica. *J. Geomagn. Geoelectr.*, **40**, 763–781.
- EJIRI, M., ONO, T., OGUTI, T., YAJIMA, N., KAMEDA, Y., HAMADA, H. and KOMATSU, K. (1988b): Visible auroral television camera for the sounding rockets S-310JA-8, -9 and -10. *J. Geomagn. Geoelectr.*, **40**, 783–797.
- EJIRI, M., ONO, T., HIRASAWA, T. and OGUTI, T. (1988c): Auroral images and particle precipitations observed by S-310JA-8, -9 and -10 at Syowa Station. *J. Geomagn. Geoelectr.*, **40**, 799–815.
- GATTINGER, R. L., HARRIS, F. R. and VALLANCE JONES, A. (1985): The height, spectrum and mechanism of type B red aurora as its bearing on the excitation of O(1S) in aurora. *Planet. Space Sci.*, **33**, 207–221.
- GERDJIKOVA, M. D. and SHEPHERD, G. G. (1987): Evaluation of auroral 5577-Å excitation processes using intercosmos Bulgaria 1300 satellite measurements. *J. Geophys. Res.*, **92**, 3367–3374.
- GILMOLE, F. R., LAHER, R. R. and ESPY, P. J. (1992): Franck-Condon factors, r -centroids, electronic transition moments, and Einstein coefficients for many nitrogen and oxygen band systems. *J. Phys. Chem. Ref. Data*, **21**, 1005–1107.
- HEDIN, A. E. (1983): A revised thermospheric model based on mass spectrometer and incoherent scatter data: MSIA-83. *J. Geophys. Res.*, **88**, 10170–10188.
- HEDIN, A. E. (1987): MSIS-86 thermospheric model. *J. Geophys. Res.*, **92**, 4649–4662.
- ITIKAWA, Y. and ICHIMURA, A. (1990): Cross sections for collisions of electrons and photons with atomic oxygen. *J. Phys. Chem. Ref. Data*, **19**, 637–651.
- ITIKAWA, Y., HAYASHI, M., ICHIMURA, A., ONDA, K., SAKIMOTO, K., TAKAYANAGI, K., NAKAMURA, M., NISHIMURA, H. and TAKAYANAGI, T. (1986): Cross sections for collisions of electrons and photons with nitrogen molecules. *J. Phys. Chem. Ref. Data*, **15**, 985–1010.
- ITIKAWA, Y., ICHIMURA, A., ONDA, K., SAKIMOTO, K., TAKAYANAGI, K., HATANO, Y., HAYASHI, M., NISHIMURA, H. and TSURUBUCHI, S. (1989): Cross sections for collisions of electrons and photons with oxygen molecules. *J. Phys. Chem. Ref. Data*, **18**, 23–42.
- JACKMAN, C. H. and GREEN, A. E. S. (1979): Electron impact on atmospheric gases. 3. Spatial yield spectra for N₂. *J. Geophys. Res.*, **84**, 2715–2724.
- LINK, R. (1992): Feautrier solution of the electron transport equation. *J. Geophys. Res.*, **97**, 159–169.
- MEYER, J. A., SETSER, D. W. and STEDMAN, D. H. (1969): Excitation of the auroral green line of atomic oxygen ($^1S \rightarrow ^1D$) by N₂(A $^3\Sigma_u^+$). *Astrophys. J.*, **157**, 1023–1025.
- ONDA, K. and ITIKAWA, Y. (1995): Simulation of particle precipitation and emission processes in electron auroras. *Proc. NIPR Symp. Upper Atmos. Phys.*, **8**, 24–36.
- ONDA, K., HAYASHI, M. and TAKAYANAGI, K. (1992): Monte Carlo calculation of ionization and

- excitation rates in electron aurora. ISAS Rep., **645**, 1–38.
- OPAL, C. B., PETERSON, W. K. and BEATY, E. C. (1971): Measurements of secondary-electron spectra produced by electron impact ionization of a number of simple gases. *J. Chem. Phys.*, **55**, 4100–4106.
- OPAL, C. B., BEATY, E. C. and PETERSON, W. K. (1972): Tables of secondary-electron production cross sections. *Atomic Data*, **4**, 209–253.
- PARKINSON, T. D. and ZIPF, E. C. (1970): Energy transfer from $N_2(A^3\Sigma_u^+)$ as a source of $O(^1S)$ in the aurora. *Planet. Space Sci.*, **18**, 895–900.
- REES, M. H. (1963): Auroral ionization and excitation by incident energetic electrons. *Planet. Space Sci.*, **11**, 1209–1218.
- REES, M. H. (1969): Auroral electrons. *Space Sci. Rev.*, **10**, 413–441.
- REES, M. H. (1987): Modelling of the heating and ionizing of the polar thermosphere by magnetospheric electron and ion precipitation. *Phys. Scrip.*, **T18**, 249–255.
- REES, M. H. and ROBLE, R. G. (1975): Observations and theory of the formation of stable auroral red arcs. *Rev. Geophys. Space Phys.*, **13**, 201–242.
- SERGIENKO, T. I. and IVANOV, V. E. (1993): A new approach to calculate the excitation of atmospheric gases by auroral electron impact. *Ann. Geophys.*, **11**, 717–727.
- SHEPHERD, M. G., MCCONNELL, J. C., TOBISKA, W. K., GLADSTONE, G. R., CHARABARTI, S. and SCHMIDTKE, G. (1995): Inference of atomic oxygen concentration from remote sensing of optical aurora. *J. Geophys. Res.*, **100**, 17415–17428.
- SOLOMON, S. C. (1991): Optical aeronomy. *Rev. Geophys. Suppl.*, **29**, 1089–1109.
- SOLOMON, S. C. (1993): Auroral electron transport using the Monte Carlo method. *Geophys. Res. Lett.*, **20**, 185–188.
- SOLOMON, S. C., HAYS, P. B. and ABREU, V. J. (1988): The auroral 6300 Å emission: Observation and modeling. *J. Geophys. Res.*, **93**, 9867–9882.
- STREIT, G. E., HOWARD, C. J., SCHMELTEKOPF, A. L., DAVIDSON, J. A. and SCHIFF, H. I. (1976): Temperature dependence of $O(^1D)$ rate constants for reactions with O_2 , N_2 , CO_2 , O_3 and H_2O . *J. Chem. Phys.*, **65**, 4761–4764.
- STRICKLAND, D. J., BOOK, D. L., COFFEY, T. P. and FEDDER, J. A. (1976): Transport equation techniques for the deposition of auroral electrons. *J. Geophys. Res.*, **81**, 2755–2764.
- TAKAYANAGI, K. (1984): A numerical study of artificial electron aurora experiment. ISAS Rep., **611**, 1–32.
- TORR, M. R. and TORR, D. G. (1982): The role of metastable species in the thermosphere. *Rev. Geophys. Space Phys.*, **20**, 91–144.
- YUROVA, I. Y. and IVANOV, V. E. (1989): *Electron Cross Sections of Atmospheric Gases*. Leningrad, “Nauka” (in Russian).

(Received March 8, 1996; Revised manuscript accepted August 30, 1996)